Microbubbles and Microparticles are Not Faithful Tracers of Turbulent Acceleration

Varghese Mathai,[1] Enrico Calzavarini,[2,*] Jon Brons,[1,3] Chao Sun,[4,1,†] and Detlef Lohse[1,5]
[1]Physics of Fluids Group, Faculty of Science and Technology, J. M. Burgers Centre for Fluid Dynamics, University of Twente, P.O. Box 217, 7500 AE Enschede, The Netherlands
[2]Université de Lille, CNRS, FRE 3723, LML, Laboratoire de Mécanique de Lille, F 59000 Lille, France
[3]Applied Mathematics Research Centre, Faculty of Engineering and Computing, Coventry University, Priory Street, Coventry CV1 5FB, United Kingdom
[4]Center for Combustion Energy and Department of Thermal Engineering, Tsinghua University, 100084 Beijing, China
[5]Max Planck Institute for Dynamics and Self-Organization, 37077 Göttingen, Germany
(Received 16 February 2016; published 8 July 2016)

We report on the Lagrangian statistics of acceleration of small (sub-Kolmogorov) bubbles and tracer particles with Stokes number $\mathrm{St} \ll 1$ in turbulent flow. At a decreasing Reynolds number, the bubble accelerations show deviations from that of tracer particles; i.e., they deviate from the Heisenberg-Yaglom prediction and show a quicker decorrelation despite their small size and minute St. Using direct numerical simulations, we show that these effects arise due the drift of these particles through the turbulent flow. We theoretically predict this gravity-driven effect for developed isotropic turbulence, with the ratio of Stokes to Froude number or equivalently the particle drift velocity governing the enhancement of acceleration variance and the reductions in correlation time and intermittency. Our predictions are in good agreement with experimental and numerical results. The present findings are relevant to a range of scenarios encompassing tiny bubbles and droplets that drift through the turbulent oceans and the atmosphere. They also question the common usage of microbubbles and microdroplets as tracers in turbulence research.

DOI: 10.1103/PhysRevLett.117.024501

Heavy and light particles caught up in turbulent flows often behave differently from fluid tracers. The reason for this is usually the particles's inertia, which can cause them to depart from fluid streamlines and distribute nonhomogeneously even when the carrier flow is statistically homogeneous [1–11]. Numerical studies have captured several interesting effects of particle inertia through point-particle simulations in homogeneous isotropic turbulence [7,12–14]. For instance, with increasing inertia, light particles showed an initial increase in acceleration variance (up to a value $\langle a^2 \rangle \sim 9$ times the tracer value) followed by a decrease, while heavy particles showed a monotonic trend of decreasing acceleration variance [15]. Such modifications of acceleration statistics arose primarily from the slow temporal response of these inertial particles, i.e., when the Stokes number St ($\mathrm{St} \equiv \tau_p/\tau_\eta$, where τ_p is the particle response time and τ_η is the Kolmogorov time scale of the flow) was finite [9,16,17]. In comparison, a lower limit of inertia can be imagined ($\mathrm{St} \ll 1$), when the particles respond to even the quickest flow fluctuations and, hence, are often deemed good trackers of the turbulent flow regardless of their density ratio [3,15,16,18]. The widespread use of small bubbles and droplets in flow visualization and particle tracking setups (e.g., hydrogen bubble visualization and droplet smoke generators) is founded on this one assumption—that $\mathrm{St} \ll 1$ renders a particle responsive to the fastest fluctuations of the flow [19–23].

In many practical situations, particles are subjected to body forces, typically gravitational or centrifugal [24]. This can be the case for rain droplets and aerosols settling through clouds, and tiny air bubbles and plankton drifting through the oceans [25,26]. The effects of gravitational settling were first brought to light through numerical studies using random and cellular flow fields [27–31]. More recently, inertial effects on settling particles were analyzed using direct numerical simulations of fully developed homogeneous isotropic turbulence [32–36]. These revealed that gravity can lead to major modifications of particle clustering, relative velocity, and pair statistics, which could be characterized as a function of St and the ratio of turbulent to gravitational acceleration: a_η/g. While the particle settling velocity and clustering were addressed widely in past studies [31,34], another crucial observable of Lagrangian turbulence is the particle's acceleration statistics (variance, correlation, and intermittency). Acceleration is important because its variance and time correlation may be linked to the energy dissipation rate, a quantity central to characterizing turbulent flows. Yet another feature unique to turbulent flows is the high level of intermittency, or deviations from Gaussian statistics. Therefore, a generic description of these quantities for rising and settling particles of arbitrary density is desirable.

In this Letter, we present the Lagrangian acceleration statistics of small air bubbles and neutrally buoyant tracer particles in a turbulent water flow where the Taylor-Reynolds number Re_λ is varied in the range 130–300. At decreasing Re_λ the bubble accelerations show deviations compared to tracer particles, which occur despite their very

small St (0.004–0.017) and small particle size. We perform Direct Numerical Simulations (DNS) of particles in homogeneous isotropic turbulence, which reveals that the deviations arise due to the drift of these particles through the turbulent flow. We develop a generic theory that predicts these gravity-induced deviations for an arbitrary-density particle, with the ratio St/Fr or equivalently the ratio of particle drift velocity to Kolmogorov velocity, as the relevant parameter controlling the deviations from ideal tracer behavior. Further, we provide insight into the modification of intermittency of particle acceleration arising due to gravity.

The experiments were performed in the Twente Water Tunnel facility, in which an active grid generated nearly homogeneous and isotropic turbulence in the measurement section [37]. The turbulent flow was characterized using the hot-film anemometry technique at different Re_λ (see Table I). Small bubbles ($\approx 150 \pm 25$ μm) were generated by blowing pressurized air through a porous ceramic plate. The particles were imaged using a high-speed camera (Photron PCI-1024) at a recording rate of 1000 fps. The camera moved on a traverse system, and illumination was provided using a 100 W pulsed laser (Litron LDY-303HE). We placed a mirror inside the tunnel at 45° inclination with the horizontal (see Fig. 1 in the Supplemental Material [38]). The laser beam was expanded into a volume, which was reflected vertically by the mirror. This crucial experimental modification from other moving camera setups [48] allowed for long particle trajectories to be recorded. We combined the conventional Gaussian-kernel smoothening method with a smoothing-spline-based technique [49,50] to obtain the higher derivatives of position data. This approach eliminated biases due to an *a priori* choice of filter windows and ensured reliable estimates of the acceleration.

We first address the question of how the bubble accelerations compare to that of similar-sized neutrally buoyant particles at different Re_λ. According to the prediction by Heisenberg and Yaglom [51], the single-component variance of acceleration should follow the relation $\langle a^2 \rangle = a_0 \epsilon^{3/2} \nu^{-1/2}$, where ϵ is the mean dissipation rate, and ν the kinematic viscosity. In Fig 1(a), we plot the Heisenberg-Yaglom constant a_0 for bubbles along with that for tracer particles. At high Re_λ, the bubbles behave similarly to tracers, with comparable a_0. However, at low Re_λ the bubbles show deviations from tracers, with an elevated a_0. The horizontal acceleration shows the greatest deviation, with $a_0 \approx 6$, while for the vertical component, $a_0 \approx 4.5$ at $\mathrm{Re}_\lambda \approx 134$. For neutrally buoyant tracer particles, a_0 is lower, ≈ 2.1 at $\mathrm{Re}_\lambda \approx 134$, and shows a marginal increase with Re_λ. Thus, the horizontal component of the acceleration variance for bubbles is almost three times that of the tracer value at the lowest Re_λ [see Fig. 1(b)]. This is also reflected in the correlation time for bubbles [Fig. 1(c) and inset], which is shorter compared with that of tracers. These deviations are surprising, since

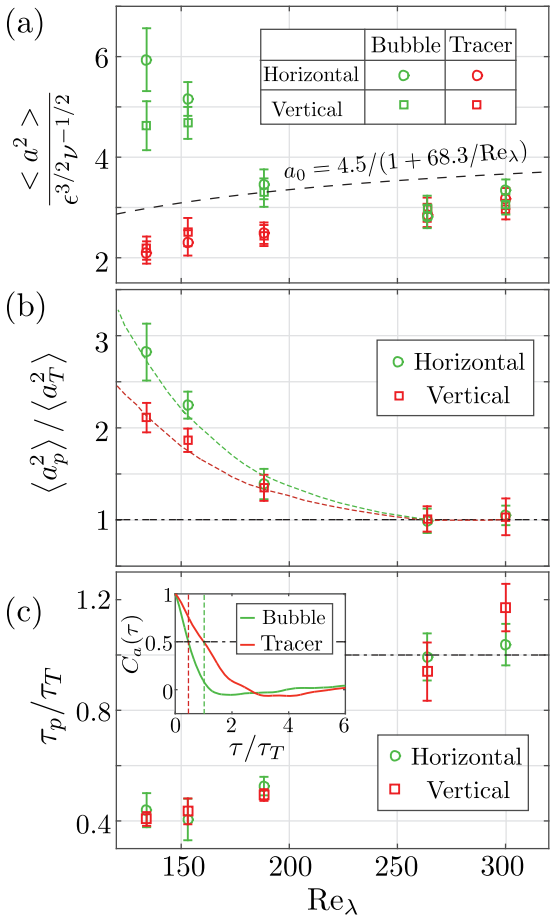

FIG. 1. (a) Heisenberg-Yaglom constant a_0, estimated for bubbles and tracer particles from experiments at different Re_λ. The dashed curve gives the a_0 estimate according to [52]. (b) Normalized acceleration variance and (c) correlation time of acceleration for bubbles vs Re_λ from experiments. $\langle a_T^2 \rangle$ is the tracer particle acceleration variance. τ_p and τ_T are defined as the 0.5 crossing time of correlation for bubbles and tracer particles, respectively. Inset: Normalized correlation function of acceleration $C_a(\tau)$ at the lowest $\mathrm{Re}_\lambda \approx 134$.

the lowest Re_λ corresponds also to the smallest St in our experiments (see Table. 1).

From Fig 1(b), we also note that the vertical component of acceleration is consistently lower as compared with the horizontal one. This anisotropy is not inherent in the carrier

TABLE I. Flow characteristics in the Twente Water Tunnel. Re_λ represents the Taylor-Reynolds number (approximate), St represents the bubble Stokes number, and a_η/g represents the ratio of turbulent to gravitational acceleration [34].

Re_λ	134	153	188	263	301
St	0.004	0.005	0.008	0.011	0.017
a_η/g	0.0016	0.0026	0.0044	0.0072	0.0141
St/Fr	4.899	4.159	3.498	2.953	2.363

flow [53] and therefore suggests the role of gravity [28]. We note that with decreasing Re_λ, the ratio of turbulent to gravitational acceleration, a_η/g, decreases in our experiments (Table 1). In order to investigate this effect in a systematic way, we perform DNS of homogeneous isotropic turbulence at $\mathrm{Re}_\lambda \approx 80$. For the particles, we use a model considering a dilute suspension of point spheres acted upon by inertial and viscous (Stokes drag) forces in the presence of gravity (see Supplemental Material [38]). We neglect lift, history, and finite-size Faxén forces, since these are verified to be negligible in the point-particle limit [15,42]. The model equation of motion for a small inertial particle advected by a fluid flow field, $(\mathbf{U}(\mathbf{X}(\mathcal{T}),\mathcal{T}))$, may be written as

$$\ddot{\mathbf{X}} = \frac{3\rho_f}{\rho_f + 2\rho_p}\left(\frac{D\mathbf{U}}{D\mathcal{T}} + \frac{12\nu}{d_p^2}(\mathbf{U}-\dot{\mathbf{X}}) + g\hat{\mathbf{e}}_z\right) - g\hat{\mathbf{e}}_z, \qquad (1)$$

where ρ_f and ρ_p are the fluid and particle mass densities, respectively, d_p is the particle diameter, and $\hat{\mathbf{e}}_z$ is the unit vector in the direction of gravity. The particles under consideration are buoyant ($0 \le \Gamma < 1$) and have a very small Stokes number ($\mathrm{St} \approx 0.05$). We vary the gravity intensity g for these particles, resulting in a range of values for a_η/g, according to the Froude number definition in [34,36]. We first address the case of bubbles ($\Gamma = 0$ in Fig. 2) at various strengths of g. With increasing g, we recover the trends observed in our experiments; i.e., the bubble acceleration variance increases. Gravity enhances the acceleration in both vertical and horizontal directions, and this is accompanied by a decrease in correlation time (see Supplemental Material [38]).

Figure 2 clearly demonstrates the role of gravity in enhancing the particle's acceleration variance. At the same time, we note that the degree of enhancement diminishes with growing Γ even at fixed a_η/g. Also, the effect of gravity on $\langle a_p^2\rangle/\langle a_T^2\rangle$ appears more pronounced in our simulations [see Fig. 1(b) and Table I]. Thus, the Froude number, if defined as a_η/g [34,36], can only give a qualitative prediction of the gravity effect. An exact prediction for an arbitrary-density particle is missing.

For a better appreciation of the contribution of gravity to the particle dynamics, we nondimensionalize Eq. (1) in terms of the Kolmogorov length η and time scales τ_η. We obtain

$$\ddot{\mathbf{x}} = \beta\frac{D\mathbf{u}}{Dt} + \frac{1}{\mathrm{St}}(\mathbf{u}-\dot{\mathbf{x}}) + \frac{1}{\mathrm{Fr}}\hat{\mathbf{e}}_z, \qquad (2)$$

where $\mathrm{St} \equiv d_p^2/(12\beta\nu\tau_\eta)$ is the Stokes number and $\mathrm{Fr} \equiv a_\eta/[(\beta-1)g]$ is a buoyancy-corrected Froude number that takes the particle density, through $\beta \equiv 3\rho_f/(\rho_f+2\rho_p)$, into account. In this situation, two important small-Stokes limits may be considered [28,35]. At high turbulence intensities ($\mathrm{Fr} \to \infty$), the third term on the right-hand side of Eq. (2) may be neglected. This leads to the well-known result $\ddot{\mathbf{x}} \simeq D_t\mathbf{u}$ for particle acceleration, where $D_t\mathbf{u}$ is the fluid tracer acceleration. However, for small Fr, the small St limit

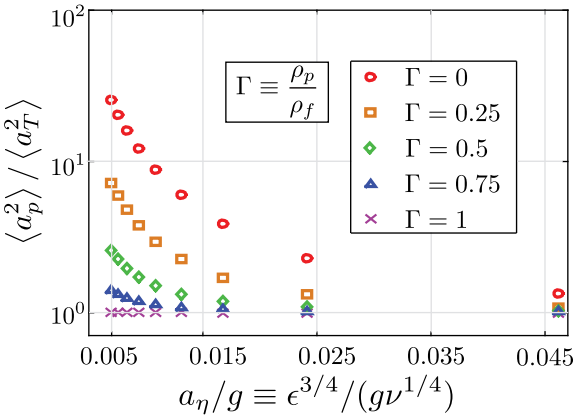

FIG. 2. Normalized horizontal acceleration variance for buoyant particles vs a_η/g obtained from Eulerian-Lagrangian DNS at $\mathrm{Re}_\lambda \approx 80$.

leads to the result $\ddot{\mathbf{x}} = D_t\mathbf{u} + (\mathrm{St}/\mathrm{Fr})\partial_z\mathbf{u}$ for particle acceleration. By employing results from homogeneous isotropic turbulence (see Supplemental Material [38]), one obtains the following relations linking the acceleration variance of particles to that of the fluid tracer:

$$\frac{\langle a_h^2\rangle}{\langle a_T^2\rangle} \equiv \frac{\langle \ddot{x}^2\rangle}{\langle (D_t u_x)^2\rangle} \simeq 1 + \frac{2}{15a_0}\left(\frac{\mathrm{St}}{\mathrm{Fr}}\right)^2, \qquad (3)$$

$$\frac{\langle a_v^2\rangle}{\langle a_T^2\rangle} \equiv \frac{\langle \ddot{z}^2\rangle}{\langle (D_t u_x)^2\rangle} \simeq 1 + \frac{1}{15a_0}\left(\frac{\mathrm{St}}{\mathrm{Fr}}\right)^2, \qquad (4)$$

where a_h and a_v are the horizontal and vertical accelerations, respectively, for an arbitrary-density particle, a_T is the tracer particle acceleration, and x and z represent the horizontal and vertical directions, respectively.

In Fig. 3, we compare the normalized acceleration variance vs St/Fr from experiment with our theoretical predictions [Eqs. (3) and (4)]. The dashed lines show the theoretical predictions using the a_0 from the present experiments [Fig. 1(a)]. The experimental data points are in reasonable agreement with our predictions. Therefore, the apparent Re_λ dependence that was seen in our water tunnel experiments (Fig. 1) is in fact a St/Fr effect, since the St/Fr increases with decreasing Re_λ in our experiments (see Table I).

The present bubble-tracking experiments cover a narrow range of $\mathrm{St/Fr} = [2\text{–}5]$ at a fixed density ratio ($\beta = 2.99$), while Eqs. (3) and (4) should be valid for an arbitrary density ratio. To test this, we compare the results of DNS for an extended range of density ratios $\beta = [0, 3]$ and $\mathrm{St/Fr} = [-10, 20]$. In Fig. 4(a), the left half ($\mathrm{St/Fr} < 0$) points to heavy particles, and the right half ($\mathrm{St/Fr} > 0$), to buoyant particles. The predicted quadratic dependence on St/Fr and even the prefactors $2/(15a_0)$ and $1/(15a_0)$ for the horizontal and vertical components, respectively, are in excellent agreement with our simulations. We note that for sufficiently large Reynolds numbers, a_0 is practically constant [51], and the ratio St/Fr becomes the sole control parameter governing the enhancement of acceleration

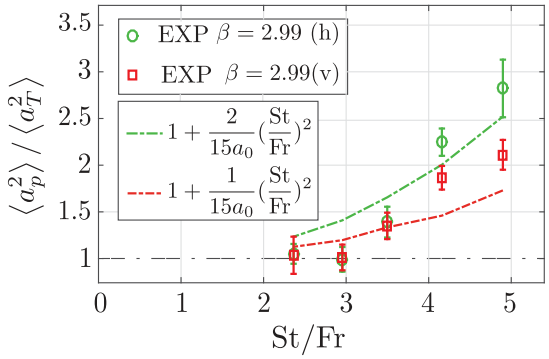

FIG. 3. Normalized acceleration variance in horizontal (h) and vertical (v) directions vs St/Fr for bubbles from our experiments. The dashed lines give the predictions based on Eqs. (3) and (4), using a_0 obtained for the tracer particles in the present experiments [Fig. 1(a)].

variance. Therefore, our results have broad applicability, to even large Re_λ atmospheric and oceanic flows. In Fig. 4(b), we present the numerical results for the tracer-normalized correlation time in the presence of gravity. We propose a model for the correlation time based on the time a particle takes to cross an energetic eddy of the flow (see Supplemental Material [38]). The model predicts a behavior of the form $\tau_p/\tau_T \approx [1/1 + k(\mathrm{St/Fr})]$, where $k \approx \sqrt[4]{(5/3\mathrm{Re}_\lambda^2)}$. The numerical results are in reasonable agreement with our predictions. Small deviations are noticeable in the small St/Fr range. In this range, the fluid acceleration $D_t\mathbf{u}$ dominates over the velocity gradient $(\mathrm{St/Fr})\partial_z\mathbf{u}$. This explains the slower decline than what is predicted by our model in the small St/Fr range (see Supplemental Material [38]). We also notice that the horizontal component (hollow symbols) is slightly higher that the vertical one (solid symbols) in the small St/Fr range. This is because the transverse velocity gradients $\partial_z u_x$ are longer correlated than the longitudinal velocity gradients $\partial_z u_z$ (see Supplemental Material [38]).

While the effects of gravity on acceleration variance and correlation time have been comprehensively demonstrated, its role on the intermittency of particle acceleration is not clear. Intermittency, i.e., the observed strong deviations from Gaussianity, can be characterized in terms of the flatness of acceleration $\mathcal{F}(a_p) \equiv \langle a_p^4 \rangle / \langle a_p^2 \rangle^2$. Assuming statistical independence between $D_t u_i$ and $\partial_z u_i$, we obtain the tracer-normalized flatness of the particle acceleration, $\mathcal{F}(a_p)/\mathcal{F}(a_T)$, as a decreasing function of St/Fr (see Supplemental Material [38]). At large St/Fr, we asymptotically approach the limits

$$\frac{\mathcal{F}(a_h)}{\mathcal{F}(a_T)} \equiv \frac{\mathcal{F}(\ddot{x})}{\mathcal{F}(D_t u_x)} \simeq \frac{\mathcal{F}(\partial_z u_x)}{\mathcal{F}(D_t u_x)}, \tag{5}$$

$$\frac{\mathcal{F}(a_v)}{\mathcal{F}(a_T)} \equiv \frac{\mathcal{F}(\ddot{z})}{\mathcal{F}(D_t u_x)} \simeq \frac{\mathcal{F}(\partial_z u_z)}{\mathcal{F}(D_t u_x)}. \tag{6}$$

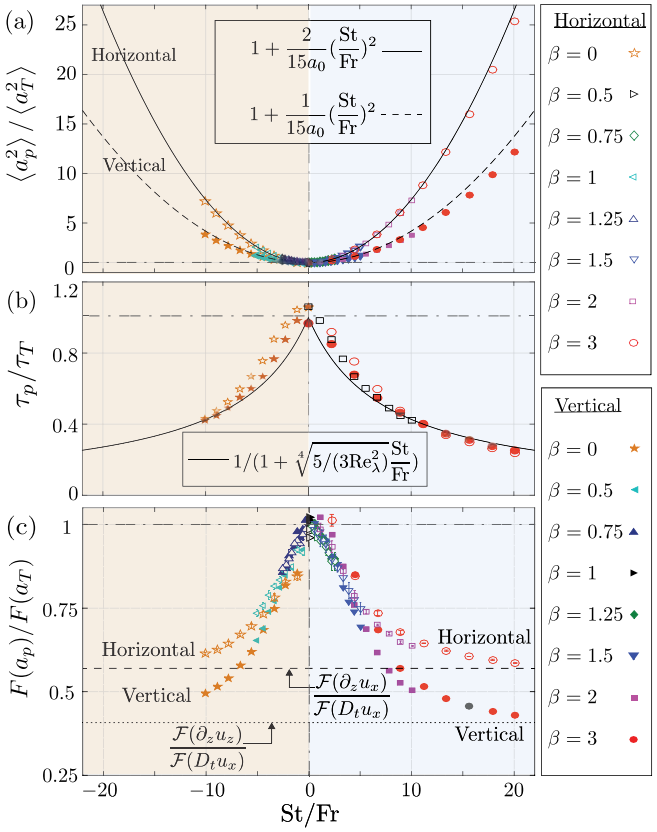

FIG. 4. (a) Normalized acceleration variance, (b) normalized correlation time, and (c) normalized flatness factor vs St/Fr for a family of buoyant and heavy particles, obtained from DNS. Solid and dashed curves in (a) show our theory predictions for horizontal and vertical accelerations, respectively [Eqs. (3) and (4)]. (b) The black curve shows the theoretical prediction for correlation time. (a)–(c) Hollow and solid symbols correspond to horizontal and vertical components, respectively.

It is verified that $\mathcal{F}(\partial_z u_z) < \mathcal{F}(\partial_z u_x) < \mathcal{F}(D_t u_x)$ [46]. This leads to the prediction $\mathcal{F}(a_v) < \mathcal{F}(a_h)$; i.e., vertical acceleration is less intermittent as compared with the horizontal one. In Fig. 4(c), we present the normalized flatness factor from our simulations for an extended (β, St/Fr) range. $\mathcal{F}(a_p)$ decreases for both buoyant and heavy particles, and the curves asymptotically reach the limits suggested by Eqs. (5) and (6). The present findings showcase the first evidence of intermittency reduction even for small St particles in turbulence.

Our results show that acceleration statistics (variance, correlation, and intermittency) is very sensitive to the ratio St/Fr. To explain the origin of this, we consider the case of a particle drifting through a turbulent flow. As the particle drifts through the flow, it meets different eddies. Owing to its short response time, the particle readjusts to the velocity of these eddies. The rate at which the particle readjusts to the new eddies is linked to the spatial velocity gradients of the turbulent flow. As a consequence, the particle experiences accelerations that the regular fluid element does not experience, thereby increasing its fluctuations (variance).

The effect becomes prominent when the drifting time of the particle past the most energetic eddies becomes shorter than the time scale of these eddies of the flow, i.e., when $\mathrm{St}/\mathrm{Fr} > 1$. This explains the scaling of the decorrelation time in Fig. 4(b) (see Supplemental Material [38] for details).

The same physical mechanisms could explain the decline in intermittency of particle acceleration. A drifting particle, instead of probing the accelerations of fluid elements, begins to sample the spatial gradients of the flow. For a turbulent flow, the intermittency of the spatial gradients of velocity is lower as compared to the intermittency of the fluid element acceleration [3,54]. Hence, the observed decline in intermittency, which asymptotically approaches the expressions given by Eqs. (5) and (6) in the limit of large St/Fr. The same qualitative behavior may be expected for moderate St particles. However, a moderate St particle responds slower to the turbulent eddies it drifts through. Hence, we expect the gravity effect to be less prominent than that for the $\mathrm{St} \ll 1$ particles we presented here, and this will be the focus of a future investigation.

In summary, the acceleration statistics of small Stokes number particles in turbulence is greatly modified in the presence of gravity. We report three major effects: an increase in acceleration variance, a decrease in correlation time, and a reduction of intermittency for buoyant and heavy particles. The ratio St/Fr governs the extent of this modification, as confirmed by our experiments using tiny air bubbles in water. Our theoretical predictions have broad validity—to particles of arbitrary density and even at large Reynolds numbers. Thus, a tiny bubble or droplet is not necessarily a good tracer of turbulent acceleration. This can be important for bubbles and droplets that drift through the turbulent oceans ($g/a_\eta \approx 100$–1000) and clouds ($g/a_\eta \approx 10$–100) [55]. On the practical side, our findings point to an important consideration when choosing bubbles or droplets for flow visualization and particle tracking in turbulent flows [19].

We gratefully acknowledge A. Prosperetti, S. S. Ray, G. D. Jin, S. Wildeman, and S. Maheshwari for insightful discussions. We thank S. Huisman, X. Zhu, P. Shukla, and V. N. Prakash for comments which helped improve our manuscript. This work was financially supported by the Simon Stevin Prize of the Technology Foundation STW of The Netherlands, European High-Performance Infrastructures in Turbulence (EUHIT), and COST action MP1305.

*enrico.calzavarini@polytech-lille.fr
†chaosun@tsinghua.edu.cn

[1] K. D. Squires and J. K. Eaton, Phys. Fluids A **3**, 1169 (1991).
[2] J. K. Eaton and J. Fessler, Int. J. Multiphase Flow **20**, 169 (1994).
[3] F. Toschi and E. Bodenschatz, Annu. Rev. Fluid Mech. **41**, 375 (2009).
[4] M. Bourgoin and H. Xu, New J. Phys. **16**, 085010 (2014).
[5] A. Wood, W. Hwang, and J. Eaton, Int. J. Multiphase Flow **31**, 1220 (2005).
[6] J. M. Mercado, D. C. Gomez, D. Van Gils, C. Sun, and D. Lohse, J. Fluid Mech. **650**, 287 (2010).
[7] R. Volk, E. Calzavarini, G. Verhille, D. Lohse, N. Mordant, J.-F. Pinton, and F. Toschi, Physica (Amsterdam) **237D**, 2084 (2008).
[8] L. Fiabane, R. Zimmermann, R. Volk, J.-F. Pinton, and M. Bourgoin, Phys. Rev. E **86**, 035301 (2012).
[9] E. Calzavarini, M. Cencini, D. Lohse, and F. Toschi, Phys. Rev. Lett. **101**, 084504 (2008).
[10] D. Lohse, Physics **1**, 18 (2008).
[11] T. Tanaka and J. K. Eaton, Phys. Rev. Lett. **101**, 114502 (2008).
[12] M. Cencini, J. Bec, L. Biferale, G. Boffetta, A. Celani, A. Lanotte, S. Musacchio, and F. Toschi, J. Turbul. **7**, N36 (2006).
[13] J. P. Salazar and L. R. Collins, Phys. Fluids **24**, 083302 (2012).
[14] V. N. Prakash, Y. Tagawa, E. Calzavarini, J. M. Mercado, F. Toschi, D. Lohse, and C. Sun, New J. Phys. **14**, 105017 (2012).
[15] E. Calzavarini, R. Volk, M. Bourgoin, E. Leveque, J. F. Pinton, and F. Toschi, J. Fluid Mech. **630**, 179 (2009).
[16] E. Calzavarini, M. Kerscher, D. Lohse, and F. Toschi, J. Fluid Mech. **607**, 13 (2008).
[17] J. Jung, K. Yeo, and C. Lee, Phys. Rev. E **77**, 016307 (2008).
[18] J. Bec, L. Biferale, G. Boffetta, A. Celani, M. Cencini, A. Lanotte, S. Musacchio, and F. Toschi, J. Fluid Mech. **550**, 349 (2006).
[19] S. Douady, Y. Couder, and M. E. Brachet, Phys. Rev. Lett. **67**, 983 (1991).
[20] C. R. Smith and R. D. Paxson, Exp. Fluids **1**, 43 (1983).
[21] L. J. Lu and C. R. Smith, Exp. Fluids **3**, 349 (1985).
[22] M. Holzner, A. Liberzon, N. Nikitin, B. Lüthi, W. Kinzelbach, and A. Tsinober, J. Fluid Mech. **598**, 465 (2008).
[23] J. M. Mercado, V. N. Prakash, Y. Tagawa, C. Sun, and D. Lohse, Phys. Fluids **24**, 055106 (2012).
[24] I. M. Mazzitelli and D. Lohse, New J. Phys. **6**, 203 (2004).
[25] G. Falkovich, A. Fouxon, and M. Stepanov, Nature (London) **419**, 151 (2002).
[26] P. Falkowski, Nature (London) **483**, S17 (2012).
[27] M. Maxey and S. Corrsin, J. Atmos. Sci. **43**, 1112 (1986).
[28] M. Maxey, J. Fluid Mech. **174**, 441 (1987).
[29] M. Maxey, Phys. Fluids **30**, 1915 (1987).
[30] M. Maxey, Phil. Trans. R. Soc. A **333**, 289 (1990).
[31] K. Gustavsson, S. Vajedi, and B. Mehlig, Phys. Rev. Lett. **112**, 214501 (2014).
[32] G. Good, P. Ireland, G. Bewley, E. Bodenschatz, L. Collins, and Z. Warhaft, J. Fluid Mech. **759**, R3 (2014).
[33] K. Chang, B. J. Malec, and R. A. Shaw, New J. Phys. **17**, 033010 (2015).
[34] J. Bec, H. Homann, and S. S. Ray, Phys. Rev. Lett. **112**, 184501 (2014).
[35] H. Parishani, O. Ayala, B. Rosa, L.-P. Wang, and W. Grabowski, Phys. Fluids **27**, 033304 (2015).
[36] P. J. Ireland, A. D. Bragg, and L. R. Collins, J. Fluid Mech. **796**, 659 (2016).
[37] V. Mathai, V. N. Prakash, J. Brons, C. Sun, and D. Lohse, Phys. Rev. Lett. **115**, 124501 (2015).

[38] See Supplemental Material at http://link.aps.org/supplemental/10.1103/PhysRevLett.117.024501, which includes Refs. [39–47], for details of the experimental setup and the theoretical predictions.
[39] M. R. Maxey and J. J. Riley, Phys. Fluids **26**, 883 (1983).
[40] R. Gatignol, J. Mec. Theor. Appl. **2**, 143 (1983).
[41] P. Spelt and A. Biesheuvel, J. Fluid Mech. **336**, 221 (1997).
[42] E. Calzavarini, R. Volk, E. Leveque, J. F. Pinton, and F. Toschi, Physica (Amsterdam) **241D**, 237 (2012).
[43] Y. Tagawa, J. M. Mercado, V. N. Prakash, E. Calzavarini, C. Sun, and D. Lohse, J. Fluid Mech. **693**, 201 (2012).
[44] J. Hinze, *Turbulence*, McGraw-Hill Series in Mechanical Engineering 2nd ed. (McGraw-Hill, New York, 1975).
[45] P. Yeung and S. Pope, J. Fluid Mech. **207**, 531 (1989).
[46] T. Ishihara, Y. Kaneda, M. Yokokawa, K. Itakura, and A. Uno, J. Fluid Mech. **592**, 335 (2007).
[47] A. Aliseda, A. Cartellier, F. Hainaux, and J. C. Lasheras, J. Fluid Mech. **468**, 77 (2002).
[48] S. Ayyalasomayajula, A. Gylfason, L. R. Collins, E. Bodenschatz, and Z. Warhaft, Phys. Rev. Lett. **97**, 144507 (2006).
[49] R. D. Brown, Z. Warhaft, and G. A. Voth, Phys. Rev. Lett. **103**, 194501 (2009).
[50] V. Mathai, M. W. Neut, E. P. van der Poel, and C. Sun, Exp. Fluids **57**, 51 (2016).
[51] A. La Porta, G. A. Voth, A. M. Crawford, J. Alexander, and E. Bodenschatz, Nature (London) **409**, 1017 (2001).
[52] R. Ni, S.-D. Huang, and K.-Q. Xia, J. Fluid Mech. **692**, 395 (2012).
[53] R. Poorte and A. Biesheuvel, J. Fluid Mech. **461**, 127 (2002).
[54] T. Ishihara, T. Gotoh, and Y. Kaneda, Annu. Rev. Fluid Mech. **41**, 165 (2009).
[55] B. Devenish *et al.*, Q. J. R. Meteorol. Soc. **138**, 1401 (2012).